(This is a sample cover image for this issue. The actual cover is not yet available at this time.)

Synthetic Metals 162 (2012) 1133–1139

Contents lists available at SciVerse ScienceDirect

Synthetic Metals

journal homepage: www.elsevier.com/locate/synmet

Study of the electrosynthesis of hollow rectangular microtubes of polypyrrole

María B. González[a], Oscar V. Quinzani[b], María E. Vela[c], Aldo A. Rubert[c], Guillermo Benítez[c], Silvana B. Saidman[a,*]

[a] Instituto de Ingeniería Electroquímica y Corrosión (INIEC), Departamento de Ingeniería Química, Universidad Nacional del Sur, Av. Alem 1253, B8000CPB Bahía Blanca, Argentina
[b] Departamento de Química, Universidad Nacional del Sur, Av. Alem 1253, B8000CPB Bahía Blanca, Argentina
[c] Instituto de Investigaciones Fisicoquímicas Teóricas y Aplicadas (INIFTA), Universidad Nacional de La Plata–CONICET, Sucursal 4 Casilla de Correo 16 (1900) La Plata, Argentina

ARTICLE INFO

Article history:
Received 7 February 2012
Received in revised form 7 May 2012
Accepted 16 May 2012

Keywords:
Polypyrrole
Microtubes
Electropolymerization
Salicylate
Steel

ABSTRACT

Hollow rectangular-sectioned microtubes of polypyrrole were deposited on stainless steel by potentiostatic electropolymerization of pyrrole in the presence of an aqueous solution of salicylate. The formed films were characterized using AFM, SEM, EDS, UV and IR spectroscopies, XRD and XPS analysis methods. The initial crystallization of salicylic acid is considered to be responsible for the formation of these special morphological structures. The experimental results indicate a high content of salicylic acid and salicylate in the electrosynthesized film. The microtubes of the polymer doped with salicylate anions coexist with the acid. PPy microtubes remain on the electrode surface after extraction of the acid from the film with ethanol.

1. Introduction

It is well known that most of the properties of conducting polymers are governed to a large extent by their structural and morphological features. The production of new morphologies of these materials with improved properties constitutes an important research area in terms of theoretical knowledge and applications. A large variety of micro- and nanostructures such as wires, tubes, cups, etc. may be synthesized either chemically or electrochemically from their respective monomers [1–3]. Among conducting polymers, polypyrrole (PPy) is one of the most promising materials for multiple applications due to numerous advantages such as its high stability and relatively simple preparation in aqueous solutions [4].

Rectangular tubes are expected to have unique properties with potential applications in the fields of electronics, optics, catalysis, and energy storage [5]. These conducting polymer structures were not frequently observed and they were prepared by chemical routes. Rectangular morphologies were observed for polyaniline [6] and poly (o-phenylenediamine) [7]. In the case of polypyrrole, it was reported the synthesis of rectangular-sectioned microtubes in aqueous solution containing β-naphthalenesulfonic acid (NSA). The template is provided by a crystalline complex formed between the monomer and NSA with a rod like structure [2,8,9]. Rectangular microtubes of PPy were also prepared by a self-assembly method using $FeCl_3$ as oxidant and Acid Red 1 (5-(acetylamino)-4-hydroxy-3-(phenylazo)-2,7-naphthalenedisulfonic acid) as dopant [10]. The formation of a complex between Acid Red 1 and Fe (II) precipitated as tetragonal crystals in the Acid Red 1 micelles conforming a template for PPy growth.

Electropolymerization has been proved to be a versatile route to synthesize PPy micro/nanotubes [11–13]. Our preliminary experiments showed, for the first time, the electrosynthesis of hollow rectangular microtubes of PPy. It was done in aqueous neutral and alkaline solutions of salicylate (Sa) [14]. A high Sa concentration in a stagnant solution is indispensable for their formation. It was tentatively proposed that microtubes were templated by salicylic acid (HSa) crystals which crystallize on the electrode surface as a result of the decrease in pH that accompanies the electrodeposition. The electropolymerization procedure has several advantages such as it allows preparing the structured PPy film in contact with the conductive substrate in a fast one-step method. This paper reports the results of a research aimed to achieve a better understanding of the formation process of the microtubes.

2. Experimental

The electrode was prepared from stainless steel 316 L rod sample which was embedded in a Teflon holder with an exposed area of 0.070 cm^2. Before each experiment, the exposed surface

* Corresponding author. Tel.: +54 291 4595182; fax: +54 291 4595182.
E-mail address: ssaidman@criba.edu.ar (S.B. Saidman).

0379-6779/$ – see front matter © 2012 Elsevier B.V. All rights reserved.
http://dx.doi.org/10.1016/j.synthmet.2012.05.013

was abraded to a 1200 grit finish using SiC, then degreased with acetone and washed with triply distilled water. Following this pretreatment, the electrode was immediately transferred to the electrochemical cell. Potentials were measured against a Ag/AgCl (3 M) electrode and a platinum sheet was used as a counter electrode. The aqueous solutions used for electropolymerization contain 0.25 M pyrrole (Py) and sodium salicylate 0.1 M, 0.2 M and 0.5 M, in a purified nitrogen gas saturated atmosphere at 25 °C. Pyrrole (Sigma–Aldrich) was freshly distilled under reduced pressure before use.

To examine the morphology of the deposits a dual stage ISI DS 130 and a Quanta 200 FEI SEMs with EDS and contact AFM in air commanded by a Nanoscope IIIa control unit from Veeco Instruments (Santa Barbara, CA, USA) were employed. Commercial SiN probes and typical forces in the range 50–220 nN were used. The surface composition was evaluated by X-ray photoelectron spectroscopy (XPS) using a Mg Kα source (1253.6 eV) XR50, Specs GmbH and a hemispherical electron energy analyzer PHOIBOS 100, Specs GmbH. A two-point calibration of the energy scale was performed using sputtered cleaned gold (Au 4f7/2, binding energy (BE) = 84.00 eV) and copper (Cu 2p3/2, BE = 932.67 eV) samples. X-ray diffraction (XRD) analysis was made using a Rigaku X-ray diffractometer (model D max III C) equipment, with CuK radiation and a graphite monochromator. Infrared spectra were recorded with a Nicolet Nexus FTIR spectrophotometer, using the KBr pellet technique. UV–vis spectra were registered on GBC-Cintra 20 equipment. Electrochemical impedance spectroscopy (EIS) measurements were done using a VoltaLab 40 Potentiostat PGZ301. The frequency used was changed from 10 kHz to 100 mHz and the signal amplitude was 10 mV.

3. Results

Salicylate concentration plays a key role in the formation of rectangular microtubes of PPy. The concentration should be higher than 0.1 M for producing this morphology. Fig. 1 shows the *i*–*t* transients during electropolymerization at 0.8 V in solutions containing 0.25 M Py and different Sa concentrations. For the solutions with the higher Sa content (0.2 and 0.5 M) after charging the double layer the current initially increases with time to a maximum value beyond which it decreases after 20 s of polarization and finally increases again at a slower rate (Fig. 1b–c). On the contrary a continuously

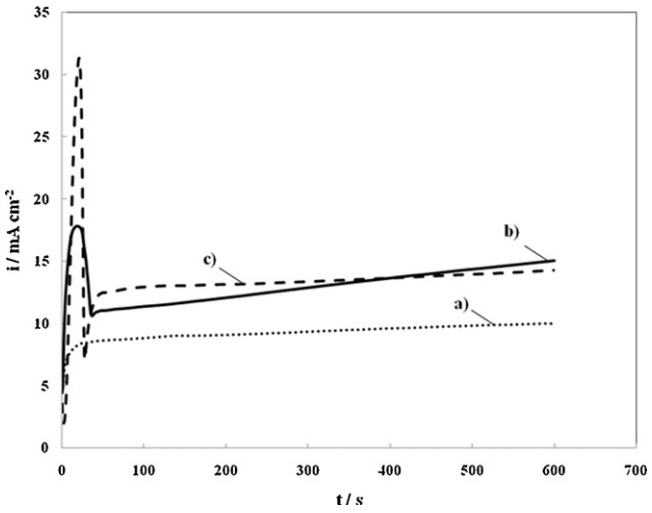

Fig. 1. Chronoamperometric curves obtained at 0.8 V in salicylate solutions containing 0.25 M Py. Salicylate concentration: (a) 0.1 M, (b) 0.2 M and (c) 0.5 M.

increasing current is registered for the lower Sa concentration (0.1 M) (Fig. 1a).

The initial stages of microtubes formation and growth can be followed by ex situ AFM. The image taken for samples prepared with 20 s of polarization reveals that the steel surface is covered by the typical granular PPy morphology (Fig. 2). The roughness of the PPy layer can be characterized by its rms (root mean square roughness) and is in the order of 250 nm for an image size of 10 μm. The value is similar to that obtained for PPy electrodeposited with another electrolyte [15]. In some regions of the sample, the coexistence of the typical cauliflower morphology of PPy with the first "blocks" of the rectangular microtubes is observed. No traces of polishing lines on steel are observed, so the crystallization of the first nucleous of microtubes cannot be attributed neither to substrate defects nor to specific morphological features of the PPy. The emergence of these first rectangular structures always leads to a decrease in the current response suggesting that they are non-conductive (Fig. 1). As electropolymerization proceeds, there is an increase in the number of growing microtubes as well as their height. This increased area of the deposit is the reason for the current rise after the maximum (Fig. 1). PPy covers the "floor" inside the tubes as well as the outer walls (Fig. 2). The cross section analysis of the microtubes

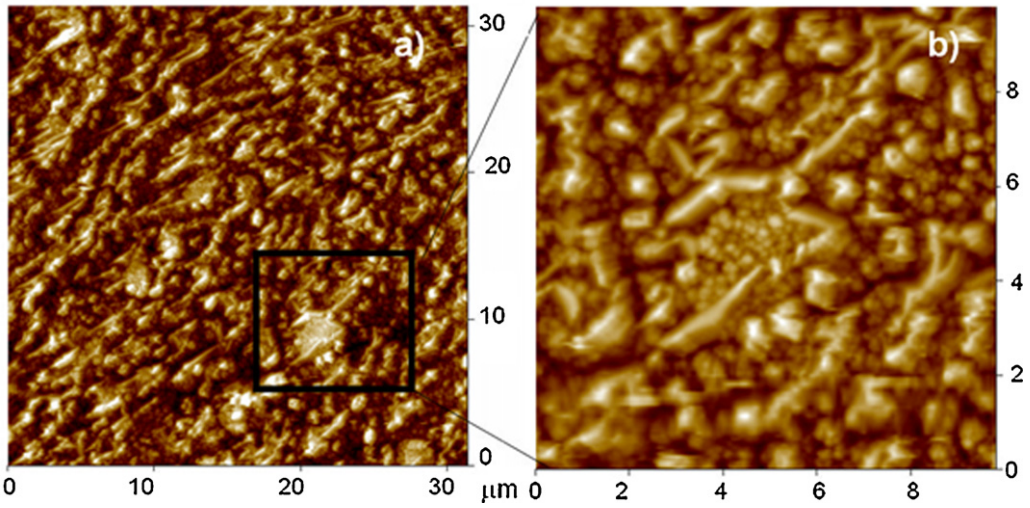

Fig. 2. AFM images of a film obtained after 20 s of electropolymerization at 0.8 V in 0.5 M salicylate solution containing 0.25 M Py. (a) Rectangular shape structures coexisting with typical cauliflower PPy structures. (b) Detail of the incipient growth of a microtube.

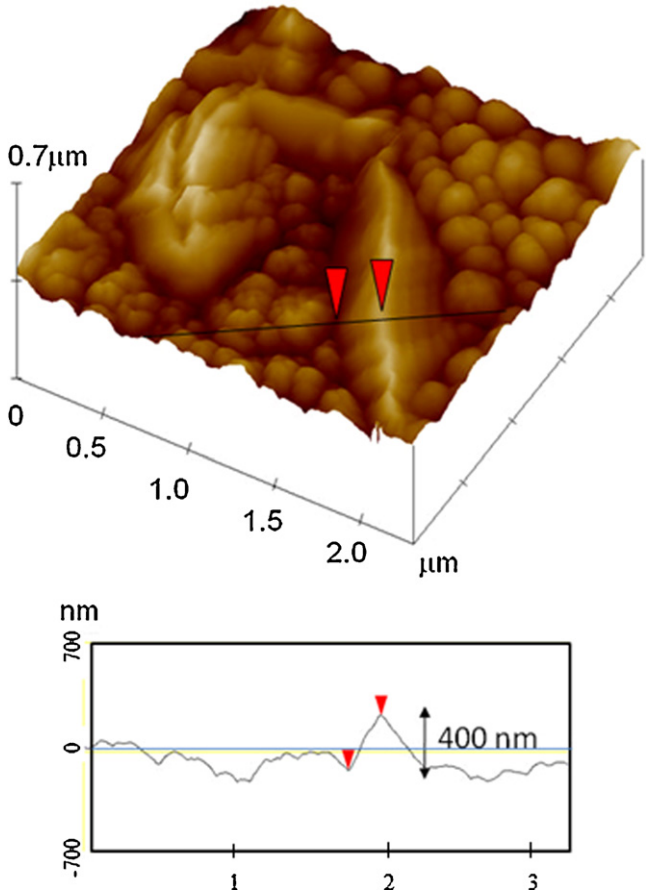

Fig. 3. 2.2 µm × 2.2 µm AFM image of a film obtained after 20 s of electropolymerization at 0.8 V in 0.5 M salicylate solution containing 0.25 M Py. The cross section shows the height of the microtube.

walls allows measuring their heights (Fig. 3). Typical values of 400–500 nm are observed for electropolymerization times of 20 s.

In order to gain more experimental evidence for the microtubes formation, SEM/EDS analysis was performed for a film synthesized at 0.8 V during 600 s in a solution containing 0.25 M Py and 0.5 M Sa. A view of the microtubes is presented in Fig. 4. It can be observed that the inner surface is smoother than the outer one. The latter

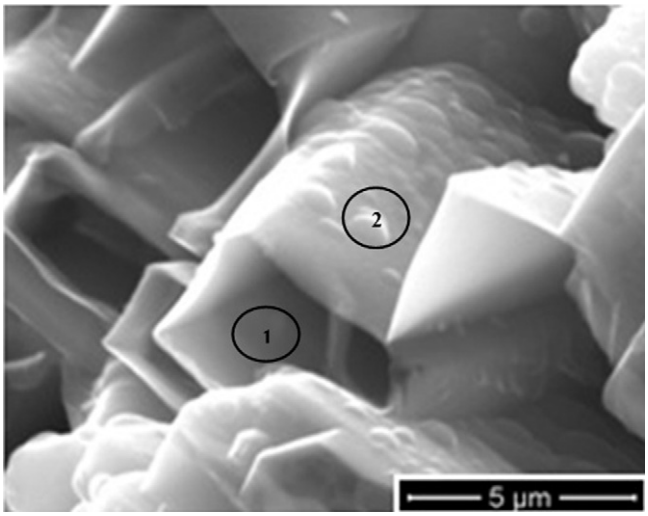

Fig. 4. SEM images of the PPy film electrosynthesized at 0.8 V in 0.5 M salicylate solution containing 0.25 M Py during 600 s.

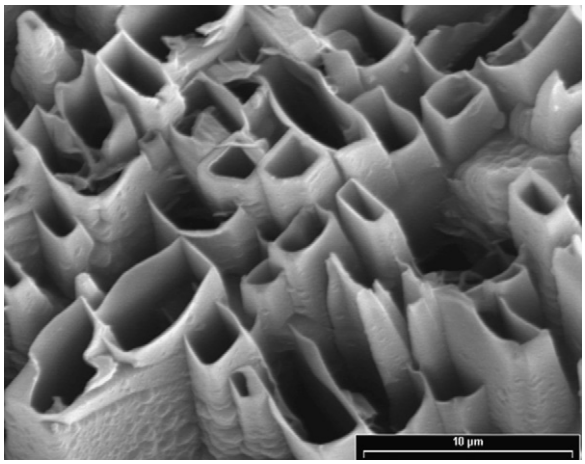

Fig. 5. SEM image of the PPy film immersed in ethanol (EtOH) during 14 days. The film was formed potentiostatically at 0.8 V during 600 s in 0.5 M salicylate solution containing 0.25 M Py.

resembles the usual granular PPy morphology. EDS analysis was performed, at points 1 and 2 on the inner and external surface of the microtube, respectively. The percentage of N is higher in the external surface (5.1%) compared to that of the inner side (0.4%), suggesting that the microtubes wall is composed of two films, the inner film consists principally of HSa, while the outer is mainly composed of PPy. No signal of Fe was detected confirming that the film completely covers the substrate.

In order to investigate the presence of HSa in the film, the recovered electrode was immersed in ethanol (EtOH) during 14 days. A SEM image of the film on the substrate indicates that microtubes morphology was not modified after this procedure (Fig. 5). On the other hand, the presence of HSa/Sa was detected in the ethanolic phase by UV spectroscopy analysis. It can be concluded that the HSa was dissolved in EtOH whereas the PPy microtubes remain on the electrode surface.

The electropolymerized film was carefully scrapped off the electrode and analyzed by IR. Its IR spectrum obtained before immersion in EtOH is presented in Fig. 6 and the assignment of bands in Table 1. The intensity and positions of the observed absorption bands are totally coincident with those of the pure solid HSa [16]. The spectrum is dominated by the strong absorption bands of the HSa solid phase crystallized in the inside walls of the microtubes

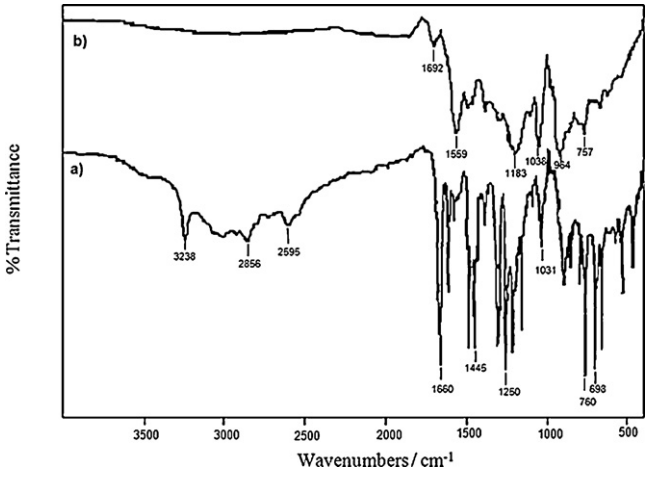

Fig. 6. FTIR spectra (KBr) of electrodeposited polypyrrole films. (a) PPy-HSa rectangular microtubes detached from the electrode surface. (b) Sa-doped PPy residue after extraction of PPy-HSa microtubes with ethanol.

Table 1
Selected IR bands (cm^{-1}) of polypyrrole films and pure HSa and NaSa.

HSa	PPy-HSa	Doped Sa-PPy	Doped Cl-PPy [15]	Sa [16]	Assignments[a]
3228s[b]	3238s				ν(OH)
3058s	3062m				ν(CC)
3007s	3006m				νas$(OH)_{COOH}$
2858s	2856m				νs$(OH)_{COOH}$
		1692m	1634s		ν(CC)
1658vs	1660vs				ν(CO)
		1559s		1582s	νas(COO)
		—	1540w		ν(CN)
		1481m		1485s	ν (CC)
		1453m	1460w		ν (CC)
1444s	1445s				ν (CC)
		1382w		1377s	ν (COO)
1325m	1324 m				ν (C(OH))
1295s	1295s				ν (CC)
		1281w		1298s	ν (CC)
1249s	1250s				ν(C—OH)$^+$ ν(C—COOH) ν(C—COOH)
		1183s	1123s		ν (CC)
1030m	1031 m				δ (CH)
		1038s	1020m		δ (CH)
		964w	903w	958s	δ (CH)
		912s			δ (CCC)
760s	760s	757w		743s	γ(CH)
698s	698s				δ (CCC)
			595vs, br		PPy chain

[a] υ: stretching; υs: symmetric stretching; υas: asymmetric stretching.
[b] br: broad, m: medium, s: strong; sh: shoulder, vw: very weak, w: weak.

(Fig. 6a). In the pure crystalline HSa the molecules are arranged as dimers through two H-bonds between the C═O bond of one molecule and the C—OH group of other molecule of the acid [17]. These molecular arrangement is maintained in the inside crystalline walls of the microtubes.

The scrapped film was immersed in EtOH during 10 days at 35 °C. A dark insoluble material remaining after extraction in EtOH which was filtered, washed, dried and then analyzed by FTIR. The spectrum (Fig. 6b) of the solid displays the vibrational bands characteristic of the oxidized state of the PPy at 1692 m and 912 s cm^{-1}. A significant displacement of these bands against the PPy films electrodeposited in acid media [18] indicates changes in the spatial disposition (packing) of the PPy chains in the outside walls of the rectangular microtubes. This effect maybe induced by the presence of the bulky Sa dopant. In the spectrum of the Sa-doped PPy films the most intense bands of the Sa anions are observed and assigned (Table 1) [19]. In addition, comparison of IR analysis produced before and after immersion in EtOH shows that the HSa signals disappear. It should be pointed out that no peak attributed to a C═O structure is observed, indicating that the polymer is not overoxidized [20].

Again, after the immersion in EtOH, the presence of HSa was detected in the ethanolic phase by UV spectroscopy analysis. The mass relationship between the HSa obtained after evaporating the EtOH and the Sa-doped polymer was ca. 1.5:1.

The voltammetric response of the covered electrode obtained before and after immersion in EtOH is presented in Fig. 7. Before immersion in EtOH the peaks in the voltammogram are poorly defined and they are superimposed on a sloping resistive line. Moreover, a large peak separation is observed. Conversely well-defined peaks with higher redox currents can be seen for the sample immersed in EtOH. This may be due to HSa dissolution that leads to a larger polymer surface exposed to the solution and to the disappearance of the ohmic resistance contribution of the non-conductive HSa. The position of the cathodic peak at negative potentials could be associated with cation transport that takes place to compensate the incomplete release of salicylate [21,22]. The redox charge corresponds to only 5% of the charge used for electropolymerization. This low value can be explained considering that the extraction of the acid is not complete. On the other hand, the integrated charges under the oxidation and reduction peaks are very similar. Thus, the coulombic efficiency over a cycle of charge–discharge is approximately 100%.

EIS data were recorded before and after immersing the coated electrode in EtOH. Measurements were performed in 0.5 M Sa at 0.0 V. The Nyquist plot before immersion showed in the low frequency region a straight line with a slope of 45° which was the characteristic feature of semi-infinite Warburg diffusion impedance. After 12 h of immersion in EtOH a finite Warburg response characterized by a nearly perfect 80° straight line in the whole frequency range was observed. Extending immersion time did not affect the impedance response. A transition from semi-infinite Warburg behavior to finite-length Warburg can be explained by considering that diffusion throughout the PPy coating replaces ion diffusion in solution [23]. This result should be

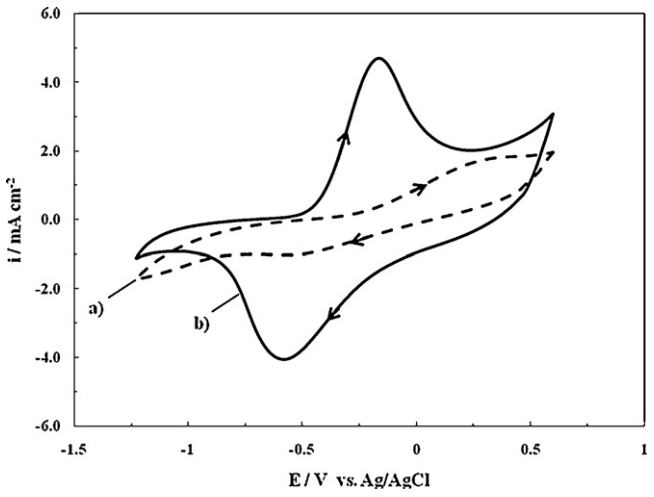

Fig. 7. Cyclic voltammograms of the PPy-covered steel electrode at 0.05 V s^{-1} in 0.5 M salicylate solution obtained before (a) and after immersion in EtOH during 3 days (b). The polymer film was electrosynthesized in the same solution containing 0.25 M Py at 0.8 V for 120 s. The 10th cycle is displayed.

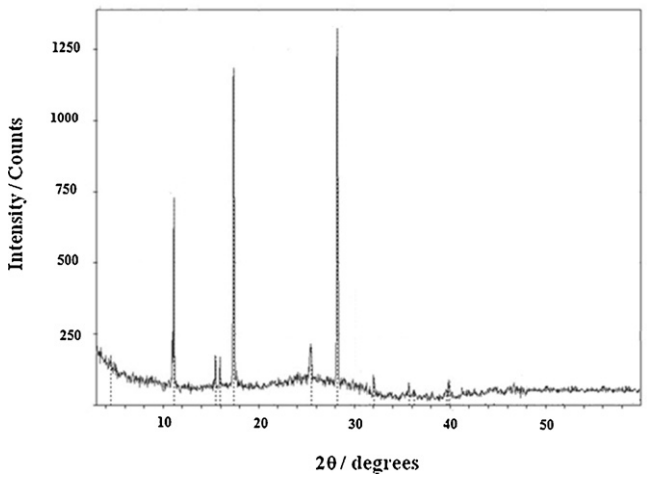

Fig. 8. X-ray spectra of PPy film obtained at 0.8 V during 600 s in 0.5 M salicylate solution containing 0.25 M Py.

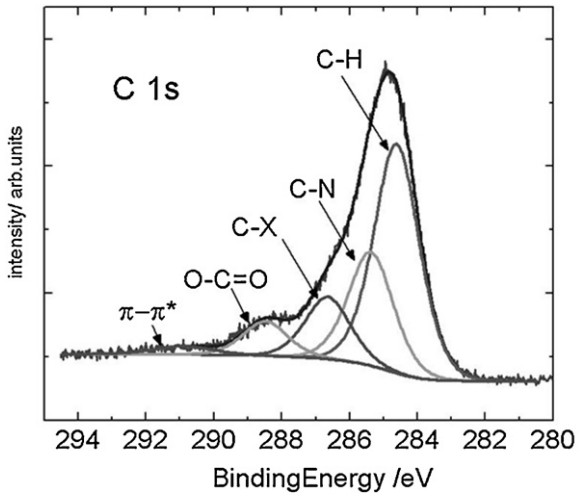

Fig. 9. C 1s XPS region and residual data analysis for a film obtained after 300 s of electropolymerization. Curve fitting components and residual data analysis are also plotted.

related with the fact that diffusion of involved species can occur in the interior of the microtubes after HSa was extracted.

The obtained film was also investigated by XRD technique (Fig. 8). The diffraction peaks related to HSa (2θ = 11.148, 17.4 and 28.245) are observed [24]. The X-ray diffraction pattern also has a broad shoulder at about $2\theta = 25^{\circ}$ indicating the amorphous behavior of the polymer as was found for the rectangular microtubes chemically synthesized [10,25].

XPS was employed to analyze the elementary composition of the film surface. The region of C 1s could be fitted by five components [26] (Fig. 9) and their assignments and percentage composition are displayed in Table 2 for samples prepared with 300 (M1) and

Table 2
Assignments and percentage composition in the C 1s region for different electropolymerization times.

Functional group	Binding energy (eV)	Fractional area (M1)	Fractional area (M2)
—CH—	284.40	60	52
C—N	285.06	17	24
C—O	286.43	13	14
O—C=O	288.45	8	8
π–π*	291.16	3	2

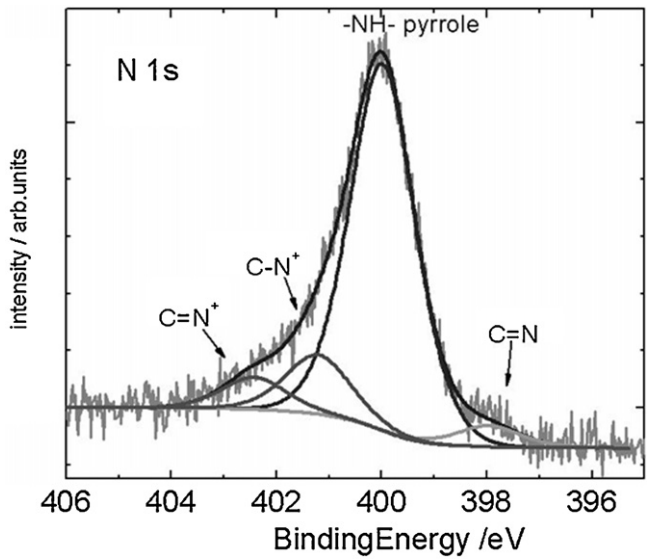

Fig. 10. N 1s XPS region and residual data analysis for a film obtained after 300 s of electropolymerization. Curve fitting components and residual data analysis are plotted.

Table 3
Assignments and percentage composition in the N 1s region for different electropolymerization times.

Functional Group	Binding energy (eV)	Fractional area (M1)	Fractional area (M2)
C=N	397.96	3	4
—NH—pyrrole	399.99	74	76
C—N^+	401.21	15	12
C=N^+	402.42	8	7

600 s (M2) of electropolymerization at 0.8 V in solutions containing 0.25 M Py and 0.5 M Sa. The components and assignments would be the following according with the literature [26,27]: 284.4 eV, the beta carbons of the pyrrolic chains and aromatic carbons of Sa/HSa (salicylate and salicylic acid) and adventitious C; 285.06 eV, the alpha carbons of pyrrole chains; 286.46 eV, C—X species where X can be the oxygen of the alcoholic functions of Sa/HSa or N of the C=N and C—N^+; 288.45 eV, the carboxylate of Sa/HSa; 291.16 eV a weak signal due to π–π* shake up satellite from the aromatic structure [27].

The N 1s region (Fig. 10) can be deconvoluted into four components with the following assignments: 397.96 eV, deprotonated N of Py; 399.99 eV, the normal N of Py; 401.21 and 401.42 eV, oxidized states of the polymer (Table 3).

The relative contributions of Sa and PPy to the composition of the surface layer can be obtained from the values reported above and they are presented in Table 4. From the values obtained of carboxylate with respect to nitrogen one can infer that the surface layer has a strong component of Sa/HSa, which lead to a mass relationship between Sa/HSa and the polymer of 1.8 and 1.4 for M1 and M2, respectively, which are close to that reported earlier in this work for the sample immersed in EtOH. The C—N/N and O—C=O/C—O

Table 4
Ratio of the different functional groups of the surface layer estimated from the areas of their XPS signals.

	M1	M2
O—C=O/N_{total}	0.86	0.65
C—N/N_{total}	1.81	2.07
O—C=O/C—O	0.82	0.72
Oxidation degree	0.23	0.19

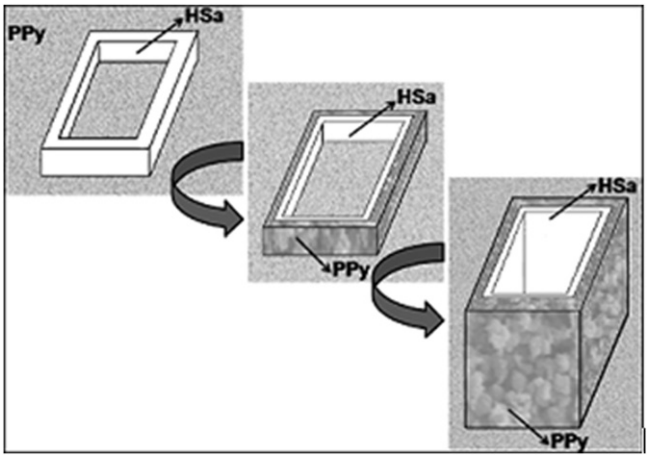

Fig. 11. Evolution of the morphology of the microtubes grown in the presence of pyrrole and salicylate anions as a function of electropolymerization time.

ratio are close to the expected ratio for Py and HSa, respectively. On the other hand, an oxidation degree of the polymer of 0.19 and 0.23 is calculated for M1 and M2 from the ratio of the peak area of positively charged nitrogen to that of the total N 1s.

4. Discussion

The experimental results indicate that the electropolymerized films with a rectangular morphology are constituted by HSa and oxidized PPy doped with Sa.

We propose that the initial crystallization of HSa on the electrode surface constitutes the building block for the formation of PPy rectangular microtubes. In a first step, only the usual globular morphology is produced (Fig. 2). Close to two H^+ ions per Py monomer polymerized are released during the polymerization process [28]. The fast generation of H^+ ions produces the protonation of Sa and at some stage HSa crystallizes on the electrode surface. At this stage the current during the potentiostatic transient decreases due to the non-conductive nature of the deposited material. On the other hand, the emergence of the HSa structures leads to a drastic morphological change because as polymerization proceeds further, the polymer is deposited at the external surface of the HSa crystals, according to AFM and SEM images. Recently, the spontaneous growth of HSa hollow whiskers when the thermal gradient exceeds a certain threshold was reported [29]. This phenomenon was explained by heat dissipation and transport of matter thanks to sublimation mechanisms and/or capillarity, i.e. by convective heat transfer. In our own experiments in an attempt to simulate the pH conditions during the electropolymerization, a 0.5 M Sa solution was acidified and the precipitated acid was isolated by filtration. SEM observations (not included) show that the crystals appear to be hollow and that dimensions of their cross section are the same as those of the PPy & HSa microtubes.

The analysis of IR spectroscopy corroborated by XRD and UV spectroscopy data indicates the presence of the acid in the film, which can be dissolved in EtOH. The IR spectrum of the remaining material is characteristic of oxidized, non degraded PPy doped with Sa anions. XPS results show that the surface layer has a strong component of Sa/HSa with respect to PPy. The doping level of the polymer is estimated from the XPS signal of the oxidized states of the polymer where values of 0.19–0.23 are obtained. The obtained results allow to propose that the existence of HSa crystals promotes a rapid PPy electrodeposition around them, ultimately producing the microtubes that once formed they grow faster than any other structure. Thus, the template is formed during electropolymerization. The top end of the polymer seems to be an active site for further polymerization and the newly formed polymer continues growing vertically to form long microtubes. As long as the electropolymerization proceeds it maintains the low pH values needed for HSa precipitation. Thus, in the microtubes the polymer coexists with the acid, the later forming the skeleton of the microtubes. The salicylate molecule is an effective dopant of the polymer. Then it plays a dual role in the process, as a dopant and as a promoter of the formation of rectangular microtubes. A scheme of our interpretation of the microtubes formation is depicted in Fig. 11.

After HSa extraction with EtOH, the microtubes of PPy doped with Sa remain intact on the electrode surface. The treatment leads to an increased electroactive surface area of the polymer.

5. Conclusions

At the early stages of polarization rectangular structures of HSa start appearing onto a granular PPy. That is, their formation occurs once the local pH decreases to a value that allows HSa crystallization. From that moment, polymer growth proceeds covering the external surface of HSa crystals. In other words, HSa crystals play a key role in tailoring the hollow rectangular-sectioned microtubes. The rectangular structures are constituted by both HSa and oxidized PPy doped with Sa anions. The removal of the acid with EtOH leads the microtubes of PPy doped with Sa intact. The hollow rectangular-sectioned microtubes have many potential applications such as their use as microcontainers and as platforms for sensors of high real area. On the other hand the possibility to change the surface charge either by the pH of the interface or by potential control opens many functionalization strategies.

Acknowledgments

The Secretaría de Ciencia y Tecnica-UNS (PGI/M111), the Consejo Nacional de Investigaciones Cientificas y Tecnicas (CONICET–PIP 112-200801-00202) and the Agencia de Promocion Cientifica (PICT 2007 no. 02308) are gratefully acknowledged for the financial support. María E. Vela is member of the research career of CIC, Pcia. Bs. As., Argentina.

References

[1] J. Heinze, B.A. Frontana-Uribe, S. Ludwigs, Chem. Rev. 110 (2010) 4724–4771.
[2] B. Schulz, I. Orgzall, I. Díez, B. Dietzel, K. Tauer, Colloids Surf., A 354 (2010) 368–376.
[3] A. Ashrafi, M.A. Golozar, S. Mallakpour, Synth. Met. 156 (2006) 1280–1285.
[4] L-X. Wang, X-G. Li, Y-L. Yang, React. Funct. Polym. 47 (2001) 125–139.
[5] C. Zhou, J. Han, R. Guo, Macromolecules 42 (2009) 1252–1257.
[6] J. Stejskal, I. Sapurina, M. Trchová, Prog. Polym. Sci. 35 (2010) 1420–1481.
[7] L. Zhang, L. Chai, H. Wang, Z. Yang, Mater. Lett. 64 (2010) 1193–1196.
[8] I. Díez, K. Tauer, B. Schulz, Colloid. Polym. Sci. 238 (2004) 125–132.
[9] I. Díez, F. Emmerling, F. Malz, C. Jäger, B. Schulz, I. Orgzall, Mater. Chem. Phys. 112 (2008) 154–161.
[10] W. Yan, J. Han, Polymer 48 (2007) 6782–6790.
[11] Ch. Jérôme, S. Demoustier-Champagne, R. Legras, R. Jérôme, Chem. Eur. J. 6 (2000) 3089–3093.
[12] C. Debiemme-Chouvy, Electrochem. Commun. 11 (2009) 298–301.
[13] S. Surdo, L.M. Strambini, C. Malitesta, E. Mazzotta, G. Barillaro, Electrochem. Commun. 14 (2012) 1–4.
[14] M.B. González, S.B. Saidman, Electrochem. Commun. 13 (2011) 513–516.
[15] S.B. Saidman, M.E. Vela, Thin Solid Films 493 (2005) 96–103.
[16] B. Humbert, M. Alnot, F. Quilès, Spectrochim. Acta A 54 (1998) 465–476.
[17] M. Boczar, L. Boda, M.J. Wójcik, Spectrochim. Acta A 64 (2006) 757–760.
[18] I.L. Lehr, O.V. Quinzani, S.B. Saidman, Mater. Chem. Phys. 117 (2009) 250–256.
[19] M. Ibrahim, A. Nada, D.E. Kamal, Indian J. Pure Appl. Phys. 43 (2005) 911–917.
[20] S. Ghosh, G.A. Bowmaker, R.P. Cooney, J.M. Seakins, Synth. Met. 95 (1998) 63–67.

[21] A.C. Cascalheira, S. Aeiyach, P.C. Lacaze, L.M. Abrantes, Electrochim. Acta 48 (2003) 2523–2529.
[22] M.J. Henderson, H. French, A.R. Hillman, E. Vieilb, Electrochem. Solid-State Lett. 2 (1999) 631–633.
[23] L. Koene, W.J. Hamer, J.H.W. de Wit, J. Appl. Electrochem. 36 (2006) 545–556.
[24] Organic and organometallic phases in International Centre for Diffraction Data, Powder Diffraction File, Newtowne Square, PA, 1994 [ICDD 14-882].
[25] J. Han, W. Yan, Y. Xu, Chem. Lett. 35 (2006) 306–307.
[26] J. Petitjean, S. Aeiyach, J.C. Lacroix, P.C. Lacaze, J. Electroanal. Chem. 478 (1999) 92–100.
[27] F. Monteil-Rivera, E.B. Brouwer, S. Masset, Y. Deslandes, J. Dumonceau, Anal. Chim. Acta 424 (2000) 243–255.
[28] S. Sadki, P. Schottland, N. Brodie, G. Sabouraud, Chem. Soc. Rev. 29 (2000) 283–293.
[29] D. Martins, T. Stelzer, J. Ulrich, G. Coquerel, Cryst. Growth Des. 11 (2011) 3020–3026.